SHEAR MODULUS OF A SATURATED GRANULAR SOIL DERIVED FROM RESONANT-COLUMN TESTS

H. Patiño
Universidad Politécnica de Madrid (UPM)
Madrid, Spain

E. Martínez
Universidad Politécnica de Madrid (UPM)
Madrid, Spain

Jesús González
Universidad Politécnica de Madrid (UPM)
Madrid, Spain
E-mail: jesus.gonzalezg@upm.es

A. Soriano
Universidad Politécnica de Madrid (UPM)
Madrid, Spain

Keywords

resonant column; resonant frequency; shear modulus; relative density; effective consolidation pressure; dynamic shear modulus

Abstract

This paper presents the results of 120 determinations of the shear modulus (G) of a saturated granular soil (20–40 Ottawa sand) in different conditions of relative density (D_r), effective consolidation pressure (σ'_c) and level of torsional excitation (T_e). The equipment used was a resonant-column apparatus manufactured by Wykeham Farrance and the tests were performed with relative density values of 20, 40, 60 and 80%, effective consolidation pressures of 50, 100, 150, 200, 250 and 300 kPa, and torsional excitations of 0.025, 0.05, 0.1, 0.2 and 0.4 volts (V), leading to shear strains (γ) between 0.002% and 0.023%. The results led to very simple empirical expressions for the shear modulus as a function of the angular strain for different effective consolidation pressures and void-ratio values.

1 INTRODUCTION

The dynamic behaviour of granular soils has been intensively studied around the world for several decades now and the results obtained from various research programs are disseminated through the proceedings of international conferences and indexed journals related to geotechnical engineering. Since there is abundant information on the dynamic behaviour of granular soils and many of the topics dealt with are commonplace; this paper will only focus on references directly related to resonant-column tests, either from the point of view of the development of the test itself or from their utilization to obtain shear-wave velocities, shear-stiffness moduli and damping ratios.

The resonant column was first used by Ishimato and Iida (1937) [1] and Iida (1938, 1940) [2, 3] to test Japanese soils, and then nearly two decades later by Bishop (1959) [4]. Since the 1960s, this technique has been widely used in many countries and has been subjected to countless modifications in the restraints applied to the specimen ends. Some of the many works on this matter are described below. For the sake of clarity, the references have been grouped by the main objective of the research rather than following a chronological order. Appearing first are the most relevant analyses of the test apparatus itself and of how to use the resonant column. Wilson and Dietrich (1960) [5] used one of the most novel – at that time – resonant columns in the USA to test clay samples. Hall and Richard (1963) [6] designed and developed a "fixed–free" resonant-column apparatus, i.e., the specimen is fixed at the base and free at the upper end, therefore allowing the soil samples to be subjected to torsional and longitudinal vibrations. Drnevich *et al.* (1966, 1967) [7, 8] developed equipment for hollow

cylindrical soil specimens, to determine the shear modulus and the damping ratio under large deformations; the reason for using hollow specimens being related to the difficulty in obtaining a representative value of the angular strain in solid samples. In addition, they developed the theory in which the interpretation of the results obtained from the resonant column test is based. The operational principle of resonant-column equipment, the calibration recommendations, the processing of the data and the interpretation of the results were clearly described by Drnevich *et al.* (1978) [9]. Menq (2003) [10] developed a resonant-column apparatus that allows testing of specimens up to 15 cm in diameter that was used to study the dynamic properties of sand and gravel. Clayton *et al.* (2009) [11] used aluminium rods of various diameters to evaluate the polar moment of inertia of the excitation system (I_o) and found that this value depended on the stiffness of the rod employed in calibrating their apparatus. However, calibrating the resonant column employed for our research led to a constant I_o value. Clayton (2011) [12] refers to some in-situ and laboratory methods to estimate the stiffness and analysed in detail factors influencing the stiffness value obtained from very-small-strain tests, like the range of strains, anisotropy and velocity of loading.

Recently, some manufacturers of equipment for obtaining dynamic parameters have marketed relatively sophisticated models for resonant column tests that allow better control and better simulation during execution of the tests; among others Wykeham Farrance in the UK, which made the device used for this investigation. A detailed description of the equipment is presented later on.

In general, the resonant column test is the most commonly used laboratory technique to measure the dynamic properties of soils subjected to a low level of deformation. The various designs developed so far imply the application of axial or torsional harmonic loads to solid or hollow specimens by means of electro-magnetic systems capable of accurately controlling the frequency and amplitude of the different types of waves that can be generated. On the other hand, Al-Sanad and Aggour (1984) [13] applied random loads and Tawfig *et al.* (1988) [14], impulsive loads.

Resonant-column tests also make it possible to determine the velocity of shear waves and to analyse their influence on other test parameters. Some researches on this point are presented below. Hardin and Richart (1963) [15] measured the shear-wave propagation velocity in samples prepared with Ottawa sand, with crushed quartz sand and with crushed quartz silts, subjected to small strains, and they proposed empirical correlations to calculate the shear modulus as a function of the void ratio and the effective consolidation pressure. Hardin (1965) [16], based on the theory of linear vibrations of a cylindrical rod, presents an expression to calculate the shear wave propagation velocity (V_s) as a function of the resonant frequency, the polar moment of inertia, the height of the specimen and the polar moment of inertia of the system. Richart *et al.* (1970) [17] proved mathematically that proportionality exists between the resonant frequency of the specimen and the corresponding shear-wave propagation velocity. Santamarina and Cascante (1996) [18] used a resonant column apparatus capable of applying both compressive and tensile deviatoric stresses to measure the velocity of shear and damping waves under small strains. These velocities turned out to depend mainly on the isotropic stress, while the deviatoric stress played a lesser role.

Probably, the factor most often analysed with this equipment has been the shear modulus, obtained in cyclic shear tests.

Kuribayashi *et al.* (1975) [19] found that the shear modulus of several materials is not a function of the relative density, but rather of the void ratio. Iwasaki *et al.* (1978) [20] present the average variation trend of the shear modulus in eight different types of sand as a function of the angular strain. In addition, they found that in the case of Toyura sand, within a wide range of deformations, a linear relationship exists between the shear modulus and the effective consolidation pressure. Tatsuoka *et al.* (1979) [21] determined that the shear modulus, within a wide range of deformations, is not affected by the initial structure of the tested specimens. Alarcón-Guzmán *et al.* (1989) [22] investigated the effect of the principal stress ratio on the shear modulus, concluding that this factor has a less important effect on the determination of the maximum shear modulus, but drastically affects the secant shear modulus. Saxena *et al.* (1989) [23] extensively reviewed empirical relations for obtaining G_{max} and the damping (D) under small strain and conducted resonant-column tests on Monterey No. 0 Sand and showed that published relations overestimated G_{max} and underestimated D for this sand. Lo Presti *et al.* (1997) [24] evaluated the influence of the strain rate in the determination of the shear modulus of granular soils, and found that this factor has a very small effect on the maximum shear modulus. Díaz-Rodríguez and López-Flores (1999) [25] proposed an empirical function (a potential expression) between the shear modulus and the isotropic consolidation stresses (σ'_c). Wichtmann and Triantafyllidis (2004) [26] analysed the influence of the history of dynamic loading on the properties of dry sands; the results thus obtained indicated that a dynamic pre-stressing moderately affects the shear modulus under small deformations. Gu *et al.* (2013) [27] used bender

elements to test three different sands subjected to small strains and found that both G_o (shear modulus) and M_0 (constraint modulus) increase with the density and the confining pressure. They found G_o to be more sensitive to E_0 (Young's modulus) and proposed empirical relations between the Poisson ratio and G_o and M_0.

Finally, some works are presented that analyse how the soil identification properties (grading, particle shape, etc.) influence results.

Chang and Ko (1982) [28] tested 23 samples of Denver sand and found that the maximum shear modulus is – to a large extent – a function of the coefficient of uniformity, whereas the effect of the mean size of the particles is minimal. Koono *et al.* (1993) [29] executed what can be regarded as a field resonant-column test in a gravel deposit. Wichtmann and Triantafyllidis (2009, 2013 and 2014) [30, 31, 32] evaluated the influence of the coefficient of uniformity and of the grain size distribution for 27 types of clean sand in the determination of the maximum shear modulus: the results obtained indicate that for equal values of the void ratio and of the effective consolidation pressure, the maximum shear modulus decreases as the coefficient of uniformity increases, whereas it does not change with the mean particle size. Martínez (2012) [33] studied the influence of the soil index properties on the determination of the dynamic parameters of a saturated granular soil. Senetakis *et al.* (2012) [34] tested sands with different grading curves, particle origin and shape under very small strains. Volcanic sands showed significantly lower G_o values than those of quartz sands, whereas their D_0 were only slightly lower compared to quartz sands.

Yang and Gu (2013) [35] found that, in the range of small strains, the shear modulus varies very little in terms of particle size.

Senetakis and Madhusudhan (2015) [36] tested quartz sands and angular-grained gravels and they proposed potential functions to relate G_o with p'. The exponent n_G was shown to be dependent on the specimen preparation procedure. Finally, Payan *et al.* (2016) [37, 38] observed that the published formulae cannot accurately relate the shear modulus under small strain with the void ratio and confining pressure, probably because the particle shape was not taken into account. Based on critical-state theories, they propose a new expression, including the effect of grading curves and particle shapes.

Taking into account the background information presented above, the objective of this investigation is an in-depth study of the influence of the relative density, effective consolidation pressure and torsional excitation values on the shear modulus of a saturated granular sand and to develop simple empirical functions to correlate these parameters.

2 MATERIAL USED

The tests were performed on 20–40 Ottawa sand (maximum, minimum and average particle sizes are 0.85, 0.43 and 0.64 mm, respectively). It is a standard material employed in many other investigations into the behaviour of granular soil. Its main characteristics are: very hard, uniform particles (the coefficient of uniformity turned out to be Cu = 1.35), fine and rounded grains and nearly pure quartz in composition.

The index properties of particles passing mesh 20 and retained in mesh 40 are as follows: specific gravity $G_s = 2.669$, maximum void ratio $e_{max} = 0.754$, and minimum void ratio $e_{min} = 0.554$. The initial properties of the specimens tested are presented in Table 1.

Table 1. Properties of specimens tested.

Relative density, D_r, %	Height, H, mm	Diameter, D, mm	Mass, g	Dry density ρ_d, g/cm^3	Void ratio, e
20	105	49.5	314.59	1.557	0.714
40	105	49.5	322.13	1.594	0.674
60	105	49.5	330.05	1.633	0.634
80	105	49.5	338.36	1.675	0.594

2.2 Description of the equipment used

The resonant-column apparatus consists of a forced oscillation system with a single torsional degree of freedom that makes the specimen vibrate within a range of frequencies in which its first natural mode can be found. In this particular investigation, the specimen remained fixed at its base and was free to vibrate at its upper end.

Testing was performed with the resonant-column device manufactured by Wykeham Farrance, Fig. 1. The frequency of the resonant-column tests is higher than 10 Hz, while in cyclic torsional shear mode the equipment typically operates at frequencies below 2 Hz. In this research, the frequency range was between 74 Hz and 140 Hz.

This instrumented and automated equipment provides a series of advantages, among which mention can be made of the following. It combines resonant-column and simple torsional shear functions. It determines automatically the resonant frequency, the shear-wave velocity, the shear modulus, the angular strain and the damping ratio, this latter parameter by using the Half-Power

Figure 1. Resonant-column apparatus manufactured by Wykeham Farrance.

method or the Free Vibration Decay method. There is no need to externally use either an oscilloscope or a function generator. The internal floating structure for the excitation system allows the execution of tests in which the specimens can experience large axial deformations during consolidation. It makes it possible to visualize, in real time, the response of the sensors during the test.

The equipment is basically constituted by two polycarbonate hollow cylindrical cells allowing, by means of the internal cell, the application of the consolidation pressure to the specimen through a fluid, without the electronic components being submerged, and – through the external cell – the application to the fluid of a confining pressure provided by a pneumatically operated system; a lower base through which the back pressure is applied and drainage of the specimen is allowed during the consolidation stage; a corrugated head piece with no possibility of drainage, to transmit the torsional forces to the specimen; a driving mechanism constituted by eight coils and four magnets to apply the torsional load to the specimen; an accelerometer attached to the mechanism to generate the torsional action and to provide the information necessary to calculate the shear-wave propagation velocity (V_s); an LVDT to measure axial deformations (with a stroke of +/- 12.5 mm and an accuracy of 0.2%), two proximity transducers to measure angular deformations in case the data supplied by the accelerometer is not used to calculate them; three pressure transducers to measure the chamber pressure (σ_c), the back pressure (B_p) and the pore water pressure (u); a transducer to register volume changes during the consolidation stage; a compact unit fitted with a power source, a manual pressure regulator, two electric pressure regulators, eight electronic components for signal conditioning and a control and data-acquisition module; and a computer for equipment control and data acquisition.

3 THEORETICAL BACKGROUND

According to the theory of torsional vibrations in a cylindrical rod, expression (1) relates the shear-wave propagation velocity (v_s) to the shear modulus (G) and to the unit mass density (ρ).

$$v_s = \sqrt{\frac{G}{\rho}} \qquad (1)$$

Expression (2), obtained by Hardin (1965) [13], calculates the shear-wave propagation velocity (v_s) as a function of the resonant frequency (F_r), the polar moment of inertia of the excitation mechanism about its symmetry axis (I_o), the polar moment of inertia of the specimen about its symmetry axis (I) and the height of the sample (h).

$$\beta \cdot \tan\beta = \frac{I}{I_0}; \text{ where } \beta = \frac{2\pi \cdot F_r \ h}{v_s} \qquad (2)$$

Implicit equation (2) can be represented graphically as a function of β, as depicted in Fig. 2.

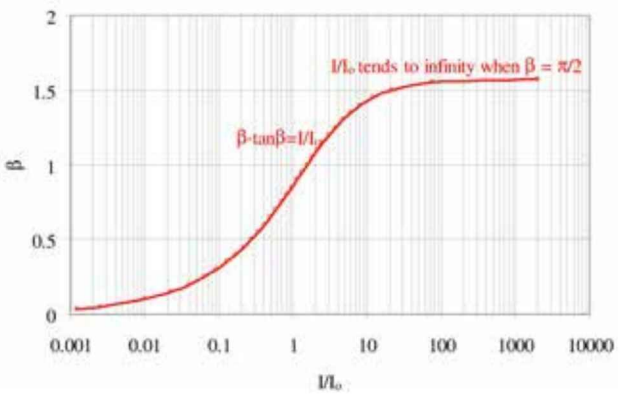

Figure 2. Graphical representation of the implicit equation (2).

Equation (3) is obtained from (1) and (2).

$$G = \frac{4\pi^2 h^2 \rho}{\beta^2} F_r^2 \qquad (3)$$

For this particular equipment the height of the specimen and the polar moment of the excitation mechanism are fixed constants. Their values are: h = 10.5 cm $I_o = 13.1 kg \cdot cm^2$.

I_o was obtained by calibration with two rods of the same dimensions and made up of different materials and turned out to be independent of the rod's stiffness. However, Clayton *et al.* (2009) [11] found that, in their equipment, I_o was dependent on the rod's stiffness. Our I_o value lies outside the range reported by them (2.99 to 4.32 $kg \cdot cm^2$) and it seems as though low values of I_o will depend on the rod's stiffness, while high I_o values will not.

The specimen diameter is D = 4.95 cm.

The densities of the samples used for this experiment range from

ρ_{sat}(min)=1.974 gr/cm^3 to ρ_{sat}(max)=2.048 gr/cm^3 or ρ_{sat} = 2.011 ± 0.037 gr/cm^3

For the central value, ρ_{sat} = 2 gr/cm^3, the value of the polar moment of inertia of the specimen is:

$$I = \frac{1}{32}\pi D^4 h \rho = 1.24 \text{ kg} \cdot \text{cm}^2 \qquad (4)$$

The corresponding value of β; obtained from equation (2)

$$\beta \cdot \text{tg}\,\beta = \frac{1.24}{13.1} = 0.0946 \text{ is} \quad \beta = 0.303 \text{ rd} \quad (\beta = 17.4^\circ)$$

The shear-wave velocity can be obtained from the resonant frequency, F_r, measured during the test

$$v_s = \frac{2\pi F_r \cdot h}{\beta} = 2.18 F_r \frac{m}{s} \quad (F_r \text{ en } H_z) \qquad (5)$$

and the corresponding value of the shear modulus $G = v_s^2 \cdot \rho = 9.51 F_r^2$ kN/m^2 (F_r en H_z).

3.1 Experimental program

This investigation was aimed at determining the effect of the relative density, the effective consolidation pressure and the magnitude of the torsional excitation on the shear modulus.

A total of 120 determinations of the resonant frequency for saturated specimens were made in specimens measuring 49.5 millimetres in diameter and 105 millimetres in height. They all had a height-to-diameter ratio equal to 2.12, thus eliminating the uncertainty related to the slenderness of the specimens; the ratio specimen diameter to particle diameter was of about 120, therefore eliminating the scale effect.

The total number of tests is a result of the combination of relative densities equal to 20, 40, 60 and 80%, effective consolidation pressures equal to 50, 100, 150, 200, 250 and 300 kPa and amplitudes of sinusoidal waves equal to 0.025, 0.05, 0.1, 0.2 and 0.4 volts. The frequency varied between 74 Hz and 140 Hz, which corresponds to angular deformations between 0.002% and 0.023%. The backpressure was equal to 400 kPa for all the tests.

3.2 Preparation and setting of specimens

The accessories depicted in Fig. 3 that are necessary for making specimens with the sedimentation method were used to carry out the tests reported herein.

Figure 3. Basic elements for the specimen preparation: 1) lifting device of the three-part mould; 2) fixed lower base; 3) porous stone; 4) three-part split mould; 5) latex membrane; 6) O-Ring; 7) O-Ring stretcher; 8) extension of three-part mould; 9) 500-cm^3 beaker with de-aired water; and 10) loading head.

The sample-preparation procedure was similar to other laboratory tests using sand. The need to reproduce specimens complying with a certain relative density led to a setting process that was very careful and repetitive.

3.3 Effect of the sample density on the ratio $\frac{G}{F_r^2}$

The value of the ratio between the shear modulus and the square of the resonant frequency, G/F_r^2, turns out to be only slightly affected by the sample density.

In fact, the theoretical value of that ratio is:

$$R = \frac{G_r}{F_r^2} = \frac{4\pi^2 h^2}{\beta^2}\rho \qquad (6)$$

When the density, ρ, increases, the value of β also increases and the result is that the value of R is almost unchanged.

In fact, taking the derivative of R with respect to ρ, we obtain:

$$\frac{dR}{d\rho} = \frac{R}{\rho} - \frac{2R}{\beta} \cdot \frac{d\beta}{d\rho} \qquad (7)$$

From equation (2), and taking the previously indicated value of I, we obtain:

$$\beta \cdot \text{tg}\,\beta = \frac{1}{32}\frac{\pi D^4 h}{I_o} \cdot \rho \qquad (8)$$

Differentiating with respect to ρ gives:

$$\frac{d\beta}{d\rho}\left(\text{tg}\,\beta + \frac{\beta}{\cos^2\beta}\right) = \frac{\beta\,\text{tg}\beta}{\rho} \qquad (9)$$

to obtain:

$$\frac{d\beta}{d\rho} = \frac{\beta}{\rho} \cdot \frac{1}{1+\alpha}; \text{ being } \alpha = \frac{2\beta}{\text{sen } 2\beta} \qquad (10)$$

and, with the help of equation (7)

$$\frac{dR}{R} = \frac{d\rho}{\rho}\left(\frac{\alpha-1}{\alpha+1}\right) \qquad (11)$$

With $\alpha > 1$, any increase in the density always produces an increase in the value of R.

For the particular case of $\rho_{sat} = 2$ gr/cm^3 equations (10) and (11) are: $\alpha = \frac{2\beta}{\text{sen } 2\beta} = 1.064$ and $\frac{dR}{R} = 0.032\ \frac{d\rho}{\rho}$. The amplitude of the range of densities for this experimental program is $\frac{\Delta\rho}{\rho} = \frac{0.037}{2} = 0.019$ and, as a consequence, the relative variation of R is: $\frac{\Delta R}{R} \cong 0.00061$.

Thus, the rationale for normalizing G with respect to F_r^2 is that, for practical purposes and for the density range of the samples tested in this investigation, the ratio G/F_r^2 can be considered to be a constant that depends on the equipment characteristics, but it does not depend on the density of the sample being tested.

4 RESULTS

The results of the 120 determinations of the resonant frequency, the angular strains measured and the values of the shear modulus G thus obtained are presented in tables 2 and 3.

Table 2. Results corresponding to relative densities equal to 20 and 40%.

σ'_c	T_e	D_r = 20%			D_r = 40%		
		F_r	G	γ	F_r	G	γ
kPa	V	Hz	MPa	%	Hz	MPa	%
50	0.025	85.5	69.2	0.004	86.6	72.2	0.005
50	0.05	84.4	67.5	0.006	85.7	70.6	0.007
50	0.1	82.6	64.6	0.009	84.1	68.1	0.011
50	0.2	80.1	60.8	0.014	82.0	64.7	0.017
50	0.4	74.7	52.8	0.019	77.2	57.4	0.023
100	0.025	105.0	104.0	0.002	107.0	110.0	0.005
100	0.05	104.0	102.0	0.004	106.0	107.0	0.007
100	0.1	102.0	98.1	0.008	106.0	107.0	0.011
100	0.2	99.7	94.1	0.014	103.0	101.0	0.016
100	0.4	95.0	85.5	0.022	99.0	94.0	0.023
150	0.025	116.0	128.0	0.003	119.0	135.0	0.004
150	0.05	115.0	126.0	0.005	118.0	132.0	0.007
150	0.1	113.0	122.0	0.009	117.0	131.0	0.010
150	0.2	111.0	117.0	0.014	115.0	126.0	0.015
150	0.4	107.0	108.0	0.022	111.0	117.0	0.022
200	0.025	125.0	147.0	0.003	128.0	155.0	0.004
200	0.05	123.0	144.0	0.005	126.0	152.0	0.006
200	0.1	122.0	142.0	0.009	126.0	151.0	0.010
200	0.2	120.0	137.0	0.014	123.0	145.0	0.015
200	0.4	117.0	129.0	0.020	120.0	137.0	0.020
250	0.025	131.0	163.0	0.003	135.0	172.0	0.004
250	0.05	130.0	160.0	0.005	134.0	170.0	0.006
250	0.1	128.0	156.0	0.009	133.0	168.0	0.009
250	0.2	127.0	153.0	0.014	131.0	162.0	0.014
250	0.4	123.0	143.0	0.019	127.0	154.0	0.017
300	0.025	137.0	178.0	0.003	141.0	188.0	0.003
300	0.05	136.0	175.0	0.005	140.0	185.0	0.005
300	0.1	135.0	174.0	0.009	139.0	183.0	0.009
300	0.2	133.0	167.0	0.014	137.0	178.0	0.014
300	0.4	129.0	158.0	0.017	134.0	171.0	0.016

Table 3. Results corresponding to relative densities equal to 60 and 80%.

σ'_c	T_e	D_r = 60%			D_r = 80%		
		F_r	G	γ	F_r	G	γ
kPa	V	Hz	MPa	%	Hz	MPa	%
50	0.025	87.4	73.4	0.005	88.8	74.7	0.003
50	0.05	84.9	69.3	0.007	87.7	72.8	0.006
50	0.1	84.1	68.1	0.010	86.6	71.1	0.009
50	0.2	80.9	63.0	0.015	83.4	66.0	0.014
50	0.4	77.7	58.0	0.022	79.0	59.2	0.020
100	0.025	104.0	104.0	0.004	109.0	113.0	0.004
100	0.05	104.0	103.0	0.007	108.0	111.0	0.006
100	0.1	103.0	101.0	0.011	107.0	108.0	0.009
100	0.2	100.0	96.3	0.016	104.0	103.0	0.014
100	0.4	96.4	88.8	0.023	100.0	94.9	0.021
150	0.025	117.0	131.0	0.004	121.0	140.0	0.004
150	0.05	117.0	129.0	0.007	120.0	136.0	0.006
150	0.1	116.0	127.0	0.010	118.0	132.0	0.009
150	0.2	114.0	123.0	0.015	117.0	130.0	0.014
150	0.4	110.0	115.0	0.022	113.0	120.0	0.021
200	0.025	126.0	152.0	0.004	131.0	163.0	0.003
200	0.05	126.0	150.0	0.006	130.0	159.0	0.006
200	0.1	125.0	148.0	0.010	128.0	155.0	0.009
200	0.2	123.0	144.0	0.015	127.0	153.0	0.013
200	0.4	120.0	136.0	0.020	123.0	144.0	0.019
250	0.025	134.0	170.0	0.004	138.0	181.0	0.003
250	0.05	133.0	168.0	0.006	137.0	179.0	0.005
250	0.1	131.0	163.0	0.009	136.0	174.0	0.009
250	0.2	130.0	161.0	0.014	134.0	171.0	0.013
250	0.4	126.0	151.0	0.018	131.0	163.0	0.017
300	0.025	140.0	187.0	0.003	145.0	198.0	0.003
300	0.05	139.0	184.0	0.006	143.0	195.0	0.005
300	0.1	138.0	180.0	0.009	142.0	191.0	0.008
300	0.2	137.0	177.0	0.014	141.0	188.0	0.013
300	0.4	133.0	167.0	0.016	136.0	175.0	0.015

Although the void ratio or the sample density is little modified under the static conditions of consolidation, at low pressures, this effect was taken into account in this research. In fact, the software implemented in the equipment evaluates the G-module from the conditions of the specimens at the end of the consolidation phase and obviously using equation (3).

The results obtained make it possible to evaluate the effect of factors such as angular strain, effective consolidation pressure and relative density in the determination of the shear modulus through the execution of the resonant-column test.

4.1 Shear modulus versus angular strain

In general, the angular strain experienced by the material increases as the level of torsional excitation increases. Fig. 4 shows this fact; however, only the results corresponding to D_r = 20% are included herein. The shear strain in Fig. 4 and 5 is the average shear strain (γ_m), obtained as $2^*\gamma_{max}/3$, where γ_{max} is the maximum shear strain measured by the accelerometer.

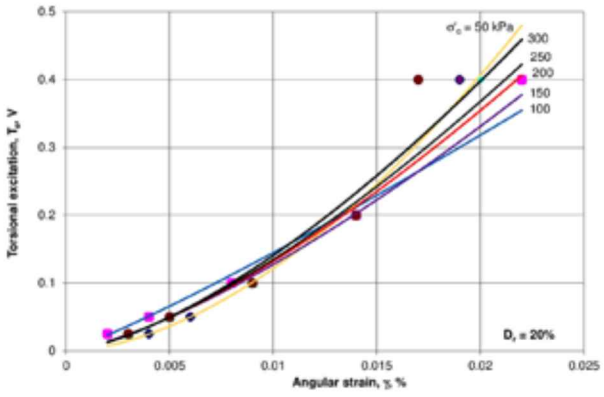

Figure 4. Typical variation trend of the angular strain as a function of the torsional excitation level, for D_r = 20%.

Fig. 6 shows the variation trends of the shear modulus as a function of the angular strains for effective consolidation pressures varying from 50 to 300 kPa and a relative density of 20%. It can be observed that in the range of small deformations (0.002–0.023%) the degradation of the shear modulus (or an increase of the inverse value of G) can be approximated as a linear function of the angular strain. This linear-type degradation recurs within the range of relative densities and effective consolidation pressures studied herein.

As these variation trends are similar, only the graphics corresponding to the relative densities equal to 20% have been included.

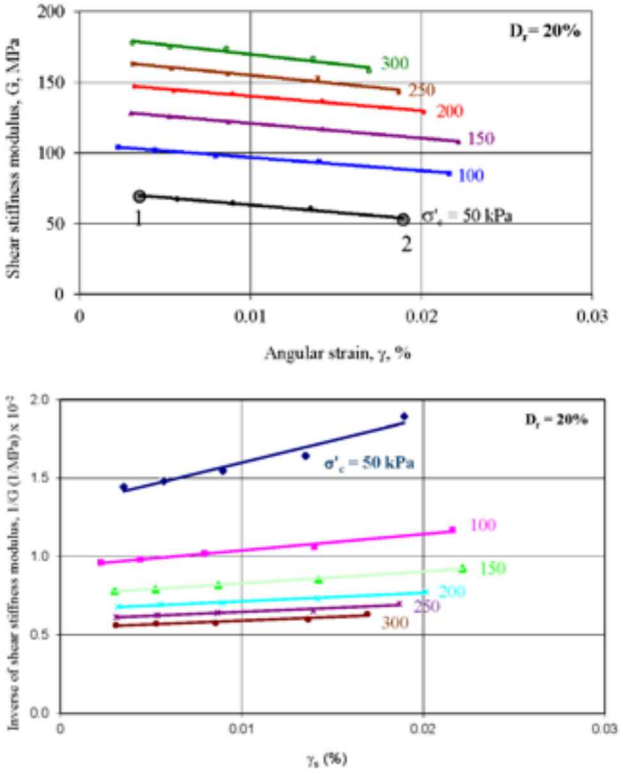

Figure 5. Typical variation trends of the shear modulus G, and its inverse 1/G as a function of the angular strain for different effective consolidation pressures and relative densities of 20%.

The degradation of the shear modulus (or the inverse of G) as a function of the angular strain has low values and reaches a maximum of 24% when the relative density is equal to 20%, the effective consolidation pressure amounts to 50 kPa and the angular strain increases from 0.0035% to 0.019% (large dots 1 and 2, Fig. 5).

The simplest mathematical model used to simulate the degradation of the shear modulus G as the strain, γ, increases is the one suggested by Hardin and Drnevich (1972) [39].

$$\frac{1}{G} = \frac{1}{G_o}\left(1 + \frac{\gamma}{\gamma_{ref}}\right) \qquad (12)$$

where G_o and γ_{ref} are the two parameters of the model.

In order to find values of G_o and γ_{ref} of the Hardin and Drnevich model that can contribute to better analyse the results of the investigation, a diagram of 1/G versus γ has been plotted and the best fit for straight lines was obtained. The resulting G_o and γ_{ref} values are given in Table 4.

Fig. 6 represents the relationship between shear modulus (G_o) and the void ratio ($\underline{e}$); in this case the void ratio is denoted by $\underline{e}$ to distinguish it from number e, the base of natural logarithms.

Table 4. Values of G_o and γ_{ref} that best fit the test results.

Value of G_o (MPa)						
D_r	Consolidation pressure σ'_c (kPa)					
	50	100	150	200	250	300
20	75.8	107.5	133.3	151.5	166.7	185.2
40	78.1	116.3	140.9	161.3	178.6	192.3
60	78.7	109.9	137.0	158.7	175.4	192.3
80	80.0	119.1	144.9	166.7	185.2	204.1

Value of γ_{ref} (%)						
D_r	Consolidation pressure σ'_c (kPa)					
	50	100	150	200	250	300
20	0.045	0.092	0.100	0.124	0.122	0.118
40	0.068	0.103	0.114	0.124	0.114	0.147
60	0.062	0.104	0.124	0.141	0.118	0.122
80	0.060	0.085	0.106	0.124	0.130	0.107

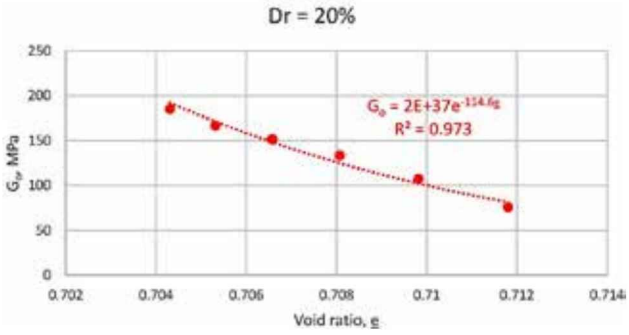

Figure 6. Value of shear modulus G_o vs void ratio (e).

As we can see in Table 4, the fact that G_o is sometimes even larger in samples with D_r = 40% than in samples with D_r = 60% is due to the narrow range of variation coupled with the unavoidable experimental scatter of results. The low sensitivity of G_o can be attributed to the nature of the sand, made of hard quartz grains (rounded and very uniform in size), which implies only little variation between the maximum and minimum void ratios.

4.2 Increase of G_o with σ'_c

The values of the shear modulus for small strains, G_o, obtained as indicated in the previous paragraph, are given in Table 4. It is clear that for each value of the relative density, the value of G_o increases as the consolidation pressure increases. See Fig. 7. Usually, the relation among these values (G_o and σ'_c) is thought to be of the type.

$$G_o = K\left(\frac{\sigma'_c}{p_o}\right)^N \cdot p_o \qquad (13)$$

where K is a "modulus number", N is an "exponent number" and p_o is the value of a standard reference pressure. For this particular investigation a value of p_o = 98.1 kPa is used.

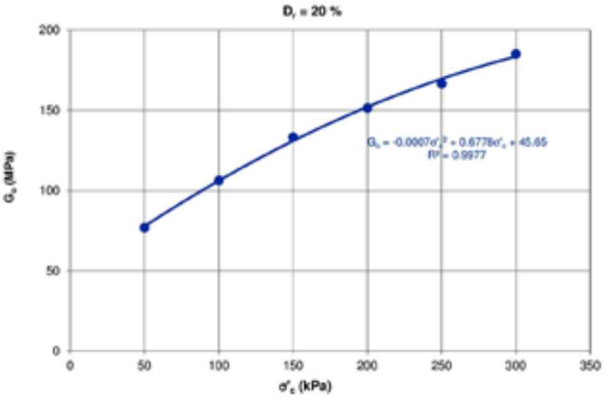

Figure 7. Values of G_o and σ'_c for D_r = 20%.

In order to investigate whether the expression (13) is applicable to this particular case, values of G were plotted versus the corresponding values of σ'_c on a log-log diagram. Fig. 8 is the plot that corresponds to D_r = 20%.

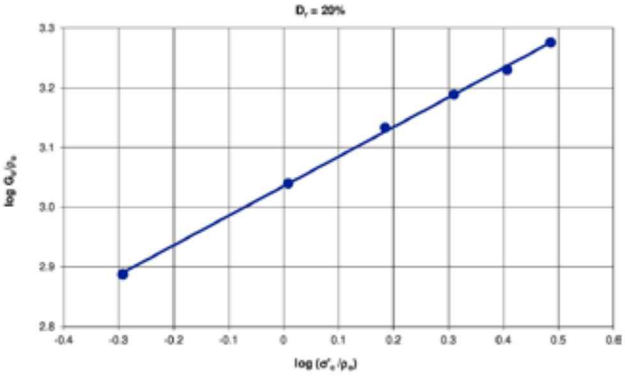

Figure 8. Double log plot of G_o and σ'_c data for D_r = 20%.

From this type of plot the model parameters can be automatically obtained from the data fit, made by minimizing the sum of the squares of the deviations of the test results that correspond to each relative density.

If the results of this research are compared to those recently obtained by Senetakis and Madhusudhan (2015) [36], Fig. 9 shows that even though the particle

Table 5. Automatically adjusted values of the dimensionless model parameters K and N.

Relative density	K	N
20 %	1084	0.495
40 %	1143	0.501
60 %	1122	0.502
80 %	1175	0.517

size differs roughly over an order of magnitude, the trend of the variation of G_o with σ'_c for the Ottawa sand coincides with that of specimen 6-2 tested by Senetakis.

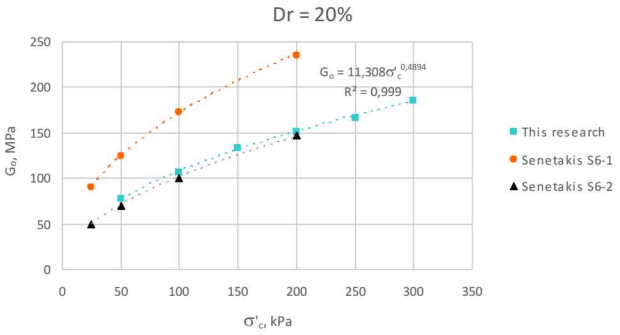

Figure 9. Values of G_o and σ'_c for D_r = 20%.

N tends to decrease slightly when the void ratio increases; it could even be suggested that N remains at a constant value of 0.50. This behaviour is different to the results obtained by Gu *et al* (2013) [27] using Toyoura sand, for which N tends to increase slightly with the void ratio. In reality, when the variation range is very narrow, some sands will show a tendency to increase N with an increase of the void ratio and in some others N will decrease slightly, as in Ottawa Sand.

4.3 Increase of γ_{ref} with σ'_c

From the values of γ_{ref} in Table 4 it seems that this parameter could be considered to be a constant but only for consolidation pressures above 200 kPa; for lower values of the consolidation pressure, the value of γ_{ref} decreases and it can no longer be considered as a constant in an hypothetical mathematical model.

A better option, which would account for the effect of large G degradation rates for lower values of the consolidation pressure, could be based on considering γ_{ref} as a variable that depends on the consolidation pressure.

It seems appropriate to assume that the degradation of the modulus G, when the angular deformation increases, should be mainly conditioned by the ratio

$$S = \frac{\tau_{\gamma\,max}}{\tau_f} \qquad (14)$$

Being $\tau_{\gamma\,max}$ the 'maximum shear stress applied' and τ_f the shear strength of the sand.

The value of $\tau_{\gamma\,max}$ can be approximated by

$$\tau_{\gamma\,max} = G\,\gamma_{max}$$

and τ_f can be estimated by

$$\tau_f \cong \sigma'_c \cdot \mathrm{tg}\,\phi$$

With these considerations, the following degradation equation can be proposed:

$$G = G_o\ (1 - A\,\frac{G\,\gamma}{\sigma_c'}) \qquad (15)$$

where A = dimensionless constant that would mainly depend on the shear strength of the tested sand, τ_f.

The value of γ_{ref} would then be given by the following expression:

$$\gamma_{ref} = \frac{\sigma_c'}{G_o \cdot A} \qquad (16)$$

Furthermore, it is known that G_o increases with the square root of σ'_c and, as a consequence, a value of γ_{ref} increasing with the square root of σ'_c should be expected.

For this reason, a value of γ_{ref} can be found to reasonably fit the data with an expression involving $(\sigma'_c/p_0)^{0.5}$. The best fit is given in Fig. 10. As we can see, the relative density also has an effect on γ_{ref}, but it is not easy to draw a clear figure showing the effect of the relative density at present.

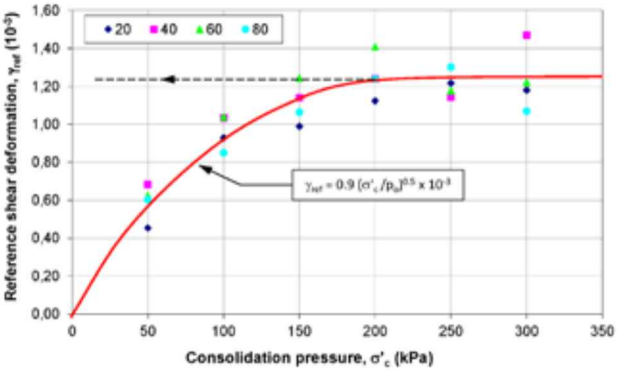

Figure 10. Reference values of the shear deformation.

This should be valid for values of γ with the interval

$$2 \times 10^{-5} < \gamma < 23 \times 10^{-5}$$

and for the range of densities of this particular investigation and for consolidation pressures lower than 200 kPa.

4.4 Influence of void ratio on the shear modulus

Four nominal values of the relative densities are used to prepare the samples for testing. These are relatively precise data, since the volume of the sample and the associated mass are known with a margin of error of about 0.1%.

During the process of consolidation some reduction in the volume takes place that increases the relative density. This change of relative density has been investigated by running an oedometer test on a sample prepared with an initial relative density of 20%. The results are given in Fig. 11.

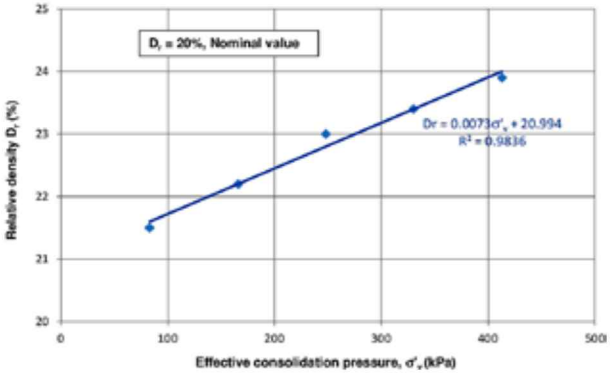

Figure 11. Increase of relative density. Oedometer test.

In resonant-column tests the consolidation pressure is applied in three directions and, as a consequence, changes in the relative density should be expected to be higher than the ones taking place in the oedometer tests, where the consolidation pressure σ'_c is only applied directly in the vertical direction. The theoretical relation of the volume changes between one-dimensional and three-dimensional consolidation is $R = 3/(1+2\,k_o)$. For this particular case and assuming an approximate value of $k_o = 0.5$, a factor $R = 1.5$ is obtained.

The real relative densities of the samples after consolidation are greater than the nominal values used in this investigation. Now, in order to better approach the effect of specimen densities, somewhat larger values of the relative densities are used.

It is known that the void ratio is a better parameter to analyze the dynamic moduli of sands than the relative density. Two different sands that have similar void ratios could have quite similar shear moduli even if their relative densities were quite different. In the same manner, two sands with equal relative densities could have quite different shear moduli.

Since the void ratio is a better parameter, the values of the relative density have been translated into void-ratio values. For this particular sand, with values of $e_{max} = 0.754$ and $e_{min.} = 0.554$, the following relation exists between the relative densities and the void ratios:

$$D_r = \frac{e_{max} - e}{e_{max} - e_{min}} = \frac{0.754 - e}{0.754 - 0.554} = \frac{0.754 - e}{0.20} \qquad (17)$$

Based on this expression and taking into consideration the small increase of the relative densities during the consolidation process of the samples, the values of the void ratios to represent the expected value of each test are given in Table 6.

Table 6. Values of the void ratio for each test series.

Relative density D_r Normal value	Relative density D_r^* Expected after consolidation	Void ratio e during the test
20%	22%	0.71
40%	42%	0.67
60%	62%	0.63
80%	82%	0.59

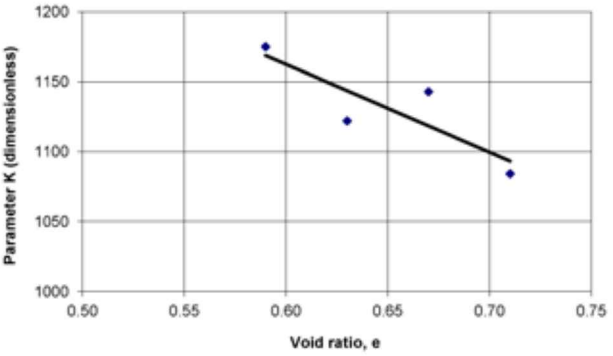

Figure 12. Value of the model modulus number K vs. void ratio, e.

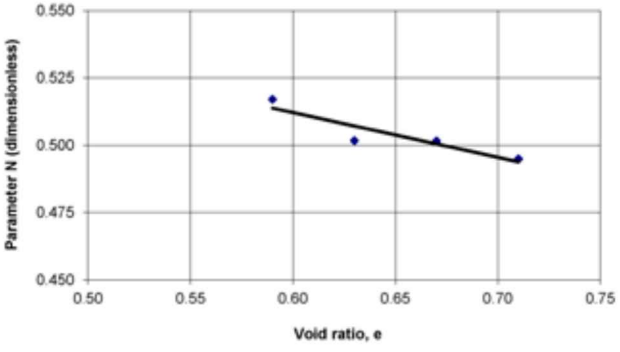

Figure 13. Value of the model modulus exponent, N, vs. void ratio, e.

Variations of the parameters K and N obtained in previous paragraphs are now plotted in Fig. 12 and Fig. 13 as a function of the void ratio.

5 DISCUSSION

The interpretation of the data obtained by testing the 120 samples of 20–40 Ottawa sand leads to proposing the following value for the shear modulus:

$$G = \left(1+\frac{\gamma}{\gamma_{ref}}\right)^{-1} \cdot k \left(\frac{\sigma'_c}{p_o}\right)^{N} \cdot p_o \qquad (18)$$

where the main variables are:

γ = angular deformation.
σ'_c = consolidation pressure

In this expression, p_o is a reference pressure with the value, p_o = 98.1 kPa = 1 kp/cm^2.

The values of the dimensionless parameters are:

$$\gamma_{ref} = 0.9 \left(\frac{\sigma'_c}{p_o}\right)^{0,5} | \times 10^{-3} \leq 1.26 \times 10^{-3} \qquad (19)$$

k = 1000 (1.54 - 0.63e)
N = 0.5 (1.22 - 0.33e)

where e = void ratio.

Senetakis and Madhusudhan (2015) [36] remarked that when relating G_o with p' through a potential function, the exponent n_G decreases slightly as the relative density increases. This research has also found that G_o can be related to σ'_c through potential functions with an exponent N that increases slightly with relative density. As mentioned, the trend in the variation of N would not necessarily be the same, as many factors are different in the various research tests. Moreover, the ranges of variation for the exponent N are very narrow. This model is considered to be valid for the range of consolidation pressures, the angular deformation and the void ratio covered for this investigation.

Those ranges are:

σ'_c : 50 to 300 kPa
γ_{max} : 2 × 10^{-5} to 23 × 10^{-5}
e: 0.59 to 0.71

Most authors, among them Richart *et al.* (1970) [11], Prakash (1981) [40], Das (1983) [41], accept that round grained sands, tested in the resonant column device in dry conditions, have a shear modulus that can be estimated using the following expression:

$$G = 697 \frac{(2.17-e)^2}{1+e} \cdot p_o \cdot \left(\frac{\sigma'_c}{p_o}\right)^{0.5} \qquad (20)$$

where e = void ratio; p_o = reference pressure (0.1 MPa) and σ'_c = consolidation pressure.

This quite famous correlation was first established by Hardin and Richart (1963) [12] and does apply to dry sands tested under resonant-column conditions with shear deformations of the order of $\gamma_{max} = 10^{-3}$ rd.

For the central value of the void ratio of this investigation, e = 0.65 and σ'_c = 150 kPa, the above expression yields the following results:

$$G = 1.207 \cdot p_o = 118 \text{ MPa}$$

From the results of this investigation it can be obtained, for the same conditions (σ'_c = 150 kPa, e = 0.65).

$$G = \left(1+\frac{\gamma}{\gamma_{ref}}\right)^{-1} \times 137 \text{ MPa} \qquad (21)$$

$$\gamma_{ref} = 1.11 \times 10^{-3}$$

It can be seen that both results would coincide if the value of γ is:

$$\gamma = 1.8 \times 10^{-4}$$

It can be concluded that the approach given in this paper agrees quite closely, at least for the central value of G, with the established practice.

This investigation deals with saturated sands, whereas the one used to make the comparison, Hardin and Richart (1963) [15], deals with dry soil. This may lead us to conclude that the effect of saturation on the value of the shear modulus could be quite small, practically negligible.

But there is one difference in respect to the influence of the void ratio on the value of the shear modulus. According to the old reference considered in this discussion [7], changing the void ratio from e = 0.71 to e = 0.59 (extreme values in this research) increases the shear modulus by 26%, irrespective of the other test variables. However, according to this investigation, the change in the modulus depends on the consolidation pressure, but it is, in any case, less than 16%.

This discrepancy could be considered as an artifact of the unavoidable imprecision of laboratory tests or it could be a real difference in behavior due to the effect of the sample saturation.

6 CONCLUSIONS

A total of 120 saturated specimens of Ottawa sand were tested in a resonant-column apparatus under angular strains (γ) of 0.002 to 0.023%, relative densities ranging from 20 to 80% and effective consolidation pressures (σ'_c) between 50 and 300 kPa. The obtained shear modulus (*G*) was related to the other intervening parameters. The main conclusions derived are as follows:

1. Relative density is the factor with the least influence on the obtained shear modulus. Following in importance are the angular strains.
2. The greatest influence in the value of the shear modulus is the effective consolidation pressure.
3. A simple empirical expression is proposed for G as a function of γ and σ'_c, for the range of γ tested.
4. For the same γ and Dr, the variation trend of G, as a function of σ'_c, can be fit to a potential function with a correlation coefficient practically equal to unity.
5. A simple expression (18) is proposed for *G*, also taking into account the void ratio (*e*) values. This research has explored a somewhat narrow range of *e* and therefore this proposal could be less precise than those made to consider other effects.
6. Although the material used was saturated Ottawa sand, the model defined in this paper might be valid in the case of other uniform granular soils with fine to medium rounded grains and quartz origin.

REFERENCES

[1] Ishimato, M., Iida, K. 1937. Determination of elastic constants of soils by means of vibration methods. Part 2. Modulus of rigidity and Poisson's ratio. Bulletin of the Earthquake Research Institute, Tokyo Imperial University, 15, 67-85.

[2] Iida, K. 1938. The Velocity of Elastic Waves in Sand. Bulletin of the Earthquake Research Institute, Tokyo Imperial University, 16, 131-144.

[3] Iida, K. 1940. On the Elastic Properties of Soil Particularly in Relation to its Water Contents. Bulletin of the Earthquake Research Institute, Tokyo Imperial University, 18, 675-690.

[4] Bishop, K.E. 1959. Forced torsional vibration of system with distributed mass and internal and external damping. Transactions of the ASME, 8-12.

[5] Wilson, S.D., Dietrich, R.J. 1960. Effect of consolidation pressure on elastic and strength properties of clay. Proceedings of the Research Conference on Shear Strength of Cohesive Soils, ASCE, Boulder, Colorado, pp. 419-435.

[6] Hall, J.R., Richard, F.E. 1963. Discussion of elastic wave energy in granular soils. ASCE, Journal of the Soil Mechanics and Foundations Division 89, 6, 27-56.

[7] Drnevich, V.P., Hall, J.R., Richart, F.E., University of Michigan, U.S. Army Engineer, Waterways Experiment Station. 1966. Large Amplitude Vibration Effects on the Shear Modulus of Sand. Vicksburg, Miss: Waterways Experiment Station. USA.

[8] Drnevich, V.P., Hall, J.R., Richart, F.E. 1967. Effect of amplitude of vibration on the shear modulus of sand. Proceedings of the International Symposium on Wave Propagation and Dynamic Properties of Earth Materials, Albuquerque, USA, pp 189-199.

[9] Drnevich, V.P., Hardin, B.O., Shippy, D.J. 1978. Modulus and damping of soils by the resonant-column method. Dynamic Geotechnical Testing, American Society for Testing and Materials 91-125.DOI: http://dx.doi.org/10.1520/STP35673S

[10] Menq, F. 2003. Dynamic properties of sandy and gravelly soils. Doctor of Philosophy Dissertation, University of Texas, Austin.

[11] Clayton, C.R.I., Priest, J.A., Bui, M., Zervos, A., Kim, S. G. 2009. The Stokoe resonant column apparatus: effects of stiffness, mass and specimen fixity. Geotechnique 59, 5, 429-437. DOI: http://dx.doi.org/10.1680/geot.2007.00096

[12] Clayton, C.R.I. 2011. Stiffness at small strain: research and practice. Geotechnique 61, 1, 5-37. DOI: http://dx.doi.org/10.1680/geot.2011.61.1.5

[13] Al-Sanad, H., Aggour, M.S. 1984. Dynamic soil properties from sinusoidal and random vibrations. Proceeding, 8th World Conference on Earthquake Engineering 3, San Francisco, pp. 15-22.

[14] Tawfiq, K.S., Aggour, M.S., Al-Samad, H.A. 1988. Dynamic properties of cohesive soils from impulse testing. Proceedings, 9th World Conference on Earthquake Engineering 3, Tokyo, pp. 11-16.

[15] Hardin, B.O., Richart, F.E. 1963. Elastic wave velocities in granular soils. ASCE, Journal of the Soil Mechanics and Foundations Division 98, 1, 33-65.

[16] Hardin, B.O. 1965. The nature of damping in sands. ASCE, Journal of the Soil Mechanics and Foundations Division 91, 1, 63-97.

[17] Richart, F.E., Hall, J.R., Woods, R.D. 1970. Vibration of Soils and Foundations. Prentice Hall, Englewood Cliffs, New Jersey.

[18] Santamarina, J. C., Cascante, G. 1996. Stress anisotropy and wave propagation: a micromechanical view. Canadian geotechnical Journal 33, 770-782. DOI: 10.1139/t96-102-323

[19] Kuribayashi, E., Iwasaki, T., Tatsuoka, F. 1975. Effects of stress-strain conditions on dynamic properties of sands. Proceedings of the Japan Society of Civil Engineers 242, 105-114. DOI: http://

dx.doi.org/10.2208/jscej1969.1975.242_105
[20] Iwasaki, T., Tatsuoka, F., Takagi, Y. 1978. Shear moduli of sands under cyclic torsional shear loading. Soils and Foundations 18, 1, 39-56. DOI: http://dx.doi.org/10.3208/sandf1972.18.39
[21] Tatsuoka, F., Iwasaki, T., Yoshida, S., Fukushima, S., Sudo, H. 1979. Shear modulus and damping by drained tests on clean sand specimen reconstituted by various methods. Soils and Foundations 19, 1, 39-54. DOI: http://dx.doi.org/10.3208/sandf1972.19.39
[22] Alarcón-Guzmán, A., Chameau, J.L., Leonards, G.A., Frost, J.D. 1989. Shear modulus and cyclic undrained behavior of sands. Soils and Foundations 29, 4, 105-119.
[23] Saxena, S., Reddy, K. 1989. Dynamic moduli and Damping ratios for Monterrey No. 0 sand by resonant column test. Soils and Foundations 29, 2, 37-51. DOI: http://doi.org/10.3208/sandf1972.29.2_37
[24] Lo Presti, D.C.F., Jamiolkowski, M., Pallara, O., Cavallaro, A., Pedroni, S. 1997. Shear modulus and damping of soils. Géotechnique 37, 3, 603-617. DOI: http://dx.doi.org/10.1680/geot.1997.47.3.603
[25] Díaz-Rodríguez, J.A., López-Flores, L. 1999. A study of microstructure using resonant-column tests. Proceeding of the Second International Conference on Earthquake Geotechnical Engineering, Lisbon, Portugal, pp. 89-94.
[26] Wichtmann, T., Triantafyllidis, T. 2004. Influence of a cyclic and dynamic loading history on dynamic properties of dry sand, part I: Cyclic and dynamic torsional prestraining. Soil Dynamics and Earthquake Engineering 24, 127-147. DOI: http://dx.doi.org/10.1016/j.soildyn.2003.10.004
[27] Gu, X.Q., Yang, J., Huang, M.S. 2013. Laboratory measurements of small strain properties of dry sands by bender element. Soils and Foundations, 53, 5, 735-745. DOI: http://dx.doi.org/10.1016/j.sandf.2013.08.011
[28] Chang, N.Y., Ko, H.Y., University of Colorado at Denver. Geotechnical Engineering Division. 1982. Effect of Grain Size Distribution on Dynamic Properties and Liquefaction Potential of Granular Soils. University of Colorado, Department of Civil and Urban Engineering, Geotechnical Engineering Division. USA.
[29] Koono, T., Suzuki, Y., Tateishi, A., Ishihara, K., Akino, K., Satsuki, I. 1993. Gravelly soil properties by field and laboratory tests. Proceedings of the 3rd International Conference on Case Histories in Geotechnical Engineering, St Louis, Missouri, 1, pp. 575-594.
[30] Wichtmann, T., Triantafyllidis, T. 2009. Influence of the Grain-Size Distribution Curve of Quartz Sand on the Small Strain Shear Modulus Gmax. ASCE, Journal of Geotechnical and Geoenvironmental Engineering 135, 10, 1404-1418. DOI: http://dx.doi.org/10.1061/(ASCE)GT.1943-5606.0000096
[31] Wichtmann, T., Triantafyllidis, T. 2013. Effect of Uniformity Coefficient on G/Gmax and Damping Ratio of Uniform to Well-Graded Quartz Sands. Journal of Geotechnical and ASCE, Geoenvironmental Engineering 139, 1, 59-72. DOI: http://dx.doi.org/10.1061/(ASCE)GT.1943-5606.0000735
[32] Wichtmann, T., Triantafyllidis, T. 2014. Stiffness and Damping of Clean Quartz Sand with Various Grain-Size Distribution Curves. ASCE, Journal of Geotechnical and Geoenvironmental Engineering, Technical Note 140, 1-4. DOI: http://dx.doi.org/10.1061/(ASCE)GT.1943-5606.0000977
[33] Martínez, E. 2012. Influencia de la densidad relativa, índice de poros, presión de consolidación y amplitud de excitación en los parámetros dinámicos de una arena saturada (Máster tesis). Universidad Complutense de Madrid.
[34] Senetakis, K., Anastasiadis, A., Pitilakis, K. 2012. The Small-Strain Shear Modulus and Damping Ratio of Quartz and Volcanic Sands. Geotechnical Testing Journal 35, 6, 964-980. DOI: http://dx.doi.org/10.1520/GTJ20120073
[35] Yang, J., Gu, X.Q. 2013. Shear stiffness of granular material at small strains: Does it depend on grain size. Géotechnique 63, 2, 165-179. DOI: http://dx.doi.org/10.1680/geot.11.P.083
[36] Senetakis, K., Madhusudhan, B. N. 2015. Dynamics of potential fill–backfill material at very small strains. Soils and Foundations 55, 5, 1196-1210. DOI: http://dx.doi.org/10.1016/j.sandf.2015.09.019
[37] Payan, M., Khoshghalb, A., Senetakis, K., Khalili, N. 2016. Effect of particle shape and validity of Gmax models for sand: A critical review and a new expression. Computers and Geotechnics 72, 28-41. Dynamics of potential fill–backfill material at very small strains. DOI: http://dx.doi.org/10.1016/j.compgeo.2015.11.003
[38] Payan, M., Denetakis, K., Khoshghalb, A., Khalili, N. 2016. Influence of particle shape on small-strain damping ratio of dry sands. Géotechnique 66, 7, 610-616. DOI: http://dx.doi.org/10.1680/jgeot.15.T.035
[39] Hardin, B.O., Drnevich, V.P. 1972. Shear Modulus and Damping in Soils: Design Equations and Curves. ASCE, Journal of the Soil Mechanics and Foundations Division 98, 7, 667-692.
[40] Prakash, S. 1981. Soil Dynamics. McGraw-Hill Book Company. USA
[41] Das, B M. 1983. Fundamentals of Soil Dynamics. Elsevier Science Publishers. USA.